Zhang, Y.; Yildirim, E.; Antila, Hanne; Valenzuela, L.S.; Sammalkorpi, Maria; Lutkenhaus, J.L.

The influence of ionic strength and mixing ratio on the colloidal stability of PDAC/PSS polyelectrolyte complexes

Published in:
Soft Matter

DOI:
10.1039/c5sm01184a

Published: 01/01/2015

Document Version
Peer reviewed version

Please cite the original version:
Zhang, Y., Yildirim, E., Antila, H., Valenzuela, L. S., Sammalkorpi, M., & Lutkenhaus, J. L. (2015). The influence of ionic strength and mixing ratio on the colloidal stability of PDAC/PSS polyelectrolyte complexes. *Soft Matter*, *11*(37), 7392-7401. https://doi.org/10.1039/c5sm01184a

Journal Name

ARTICLE

The influence of ionic strength and mixing ratio on the colloidal stability of PDAC/PSS polyelectrolyte complexes†

Received 00th January 20xx,
Accepted 00th January 20xx

DOI: 10.1039/x0xx00000x

www.rsc.org/

Yanpu Zhang, [a] Erol Yildirim, [b] Hanne S. Antila, [b] Maria Sammalkorpi, [b] Luis D. Valenzuela, [a] and Jodie L. Lutkenhaus*[a]

Polyelectrolyte complexes (PECs) form by mixing polycation and polyanion solutions together, and have been explored for a variety of applications. One challenge for PEC processing and application is that under certain conditions the as-formed PECs aggregate and precipitate out of suspension over the course of minutes to days. This aggregation is governed by several factors such as electrostatic repulsion, van der Waals attractions, hydrophobic interactions. In this work, we explore the boundary between colloidally stable and unstable complexes as it is influenced by polycation/polyanion mixing ratio and ionic strength. The polymers examined are poly(diallyldimethylammonium chloride) (PDAC) and poly(sodium 4-styrenesulfonate) (PSS). Physical properties such as turbidity, hydrodynamic size, and zeta potential are investigated as a function of time upon complex formation. We also perform detailed molecular dynamics simulations to examine the structure and effective charge distribution of the PECs at varying mixing ratios and salt concentrations to support the experimental findings. The results suggest that the colloidally stable/unstable boundary possibly marks the screening effects from added salt, resulting in weakly charged complexes that aggregate.

1. Introduction

Polyelectrolyte complexes (PECs) form when oppositely charged polymers are mixed together and the two interact to form a larger structure.[1] Promising applications of PECs range from industrial flocculants, coatings, and membranes to advanced material fields such as solar cells, injectable hydrogels, drug release, medical implants, chemical sensors, and lubricants.[2-7] PECs have been described by many works,[1, 8-15] which have shown complexation to be a largely isoenthalpic, entropy-driven process, resulting from an intricate interplay of electrostatic, van der Waals, and hydrophobic interactions. Hence, PEC formation is highly sensitive to polyelectrolyte characteristics (e.g. polymer structure and charge density) and external parameters including polyelectrolyte concentration, polyanion/polycation mixing ratio, mixing order, salt type, salt concentration, and solution pH (for weak polyelectrolytes).[8, 16-23] The resulting structure may be solid-like (complex solid) or liquid-like (complex coacervate).[24-26]

Many prior investigations have focused upon the effects of mixing ratio, ionic strength, and other external parameters on the formation or response of PECs, usually at a fixed point in time. Little attention is paid to the temporal domain, even though many PECs macroscopically change (phase separate or aggregate) over the course of minutes to days. Knowledge of PEC behaviour with respect to time is expected to be significant for any industrial application proposing the formation and implementation of PECs, especially with regard to colloidal stability.

It has been shown that under certain conditions PECs aggregate, ripen, and eventually precipitate out of suspension,[24, 27, 28] although there is limited knowledge regarding the specific boundaries that govern this behaviour. A recent review summarizes this issue from a theoretical point of view, describing aggregation to occur when short-range attractions (van der Waals, hydrophobic) overcome long-range electrostatic repulsion between like-charge complexes.[29] The process is generally described as the aggregation or bridging of primary PEC particles into larger secondary particles. At a critical point, the secondary particle precipitates and no longer remains suspended in the PEC solution, resulting in solid-liquid macrophase separation. This process is markedly different from coacervation, which is liquid-liquid phase separation. Dautzenberg and Jaeger reported that salt concentration and mixing ratio played a large role in whether or not PECs of poly(sodium 4-styrenesulfonate) (PSS) and polycation poly(diallyldimethylammonium chloride) (PDAC) and its copolymers, aggregated or flocculated, although a limited salt range was explored.[8] For nonstoichiometric ratios, the complexes consisted of spherical particles with a neutralized core and a shell of the excess component, and for stoichiometric ratios, the shell of excess was less pronounced.

Besides colloidal stability, salt concentration and mixing ratio also have been shown to strongly influence phase behaviour (solution/complex coacervate/complex solid).[24, 27, 30, 31] It is generally found that no added salt or low salt concentration

[a] Artie McFerrin Department of Chemical Engineering, Texas A&M University, College Station, Texas 77843, United States. E-mail: Jodie.lutkenhaus@tamu.edu
[b] Department of Chemistry, Aalto University, P.O. Box 16100, 00076 Aalto, Finland.
† Electronic Supplementary Information (ESI) available. See DOI: 10.1039/x0xx00000x

produces a complex solid, and that high salt concentrations excessively screen the polyelectrolytes to prevent complexation. Intermediate salt concentrations yield a coacervate, although the boundary between complex solid and complex coacervate is not definitive.[30] At even higher salt concentrations, excessive screening results in dissolved polyelectrolyte chains and the absence of PECs. Many of these findings and others[32-35] have attempted to equate the properties of PECs with that of layer-by-layer assemblies.

More recently, Schlenoff and coworkers conducted studies of PECs made from PDAC and PSS.[14, 30, 36-38] The addition of salt water rendered the PEC's processable by extrusion or ultracentrifugation, forming a class of materials termed "saloplastics".[36, 39-41] It was shown that salt type affected the doping and diffusion coefficients of the extruded PECs.[37] Salt doping also influenced the thermal transition of the saloplastic, as it modified the nature of the ion-pair interactions between the two oppositely charged polymers.[38] The solution/coacervate/precipitate boundary was also probed in a ternary PEC/water/salt phase diagram, in which the PECs were equilibrated by a "backwards" salt annealing method.[30] Here, the colloidal stability and temporal evolution of PECs are presented. Strong polyelectrolytes, PDAC and PSS are selected as the polycation and polyanion, respectively, because there is a good deal of existing literature on their PEC phase behaviour.[8, 14, 27, 30, 36, 37, 42-55] We chose to focus upon mixing ratio and ionic strength because they have a large effect on colloidal stability at a given molecular weight and total polymer concentration. Salt type was not explored here, but has been studied extensively elsewhere.[19, 56] The ionic strength (0-3 M NaCl) and mixing ratio (20 mol% to 80 mol% PDAC) are varied, and the turbidity, hydrodynamic radius, and zeta potential are recorded. Under these conditions, solid-like PECs are formed. PECs show solution behaviour ranging from a stable colloidal dispersion to an unstable aggregating precipitate and eventually dissolved polymer chains. Molecular dynamic simulations on PECs of corresponding mixing ratios and salt concentrations are conducted to obtain a microscopic view on the assembling structures and the resulting aggregation barriers that dictate their colloidal stability. The simulation findings are discussed with the experimental results.

2. Materials and Methods

2.1 Materials

In this work, poly(diallyldimethylammonium chloride) (PDAC, Mw=200,000-350,000 g/mol, 20 wt% in water, Sigma Aldrich) was chosen as the polycation, poly(sodium 4-styrenesulfonate) (PSS, Mw=500,000 g/mol, powder, Scientific Polymer Products) was chosen as the polyanion, and both were used directly without any further treatment. Sodium chloride was used to adjust the ionic strength of the solutions. The water used in all experiments was 18.2 MΩ cm (Milli-Q) water.

2.2 Polyelectrolyte complex preparation

To study the effects of polycation/polyanion mixing ratio and ionic strength on the formation of PECs, the concentration of the overall repeat unit of the polyelectrolyte was held constant at 10 mM. The PDAC solution was always added to the PSS solution, for which both had the same adjusted ionic strength. PDAC or PSS stock solutions with concentrations (based on repeat unit) of 4, 6.7, 10, 13.3, 16 mM were prepared. Five combinations of PDAC and PSS were made, specifically with mol% PDAC varying from 20% to 80% (again based, on repeat unit), as shown in Table 1. Different amounts of NaCl were added to the stock polyelectrolyte solution to adjust the ionic strength before mixing. For each polyelectrolyte solution, the ionic strength varied from 0 to 1.0 M with an interval of 0.1 M and from 1.0-3.0 M with an interval of 0.5 M. PEC formation was carried out directly in disposable polystyrene cuvettes for UV-Vis-NIR spectroscopy and dynamic light scattering (DLS) characterization. To make PDAC/PSS complexes, 0.75 mL PSS solution was first loaded into the cuvette; then 0.75 mL PDAC solution was mixed rapidly into the PSS solution using a pipette. Mixing occurred within a 1 sec time span. All PECs were prepared just prior to measurements, unless otherwise indicated.

Table 1. PDAC/PSS complex composition. All values are based on repeat unit.

Group	mol% PDAC in the PEC	PDAC concentration (mM)	PSS concentration (mM)
1	20	4	16
2	33	6.7	13.3
3	50	10	10
4	67	13.3	6.7
5	80	16	4

2.3 Turbidity measurements

A Hitachi U-4100 UV-Vis-NIR spectrophotometer (341-F) was used to measure the turbidity of PECs formed in the cuvettes. A wavelength of 750 nm was selected because both pure PDAC and PSS solutions do not absorb light at this wavelength. All PECs were analyzed just after preparation. The turbidity (T) of the mixture was calculated by

$$T = -\ln\left(\frac{I}{I_0}\right) \text{ [=] a.u.} \quad (1)$$

Where I_0 is the incident light intensity of the control solution and I is the intensity of light passed through the PEC. Turbidity was calculated in adsorption units (a.u.).[24]

2.4 Hydrodynamic size and zeta potential measurements

A Zetasizer Nano ZS90 (Malvern Instruments, Ltd., Worcestershire, UK) was employed to characterize the PEC hydrodynamic size and zeta potential. In the hydrodynamic size measurements, newly prepared PECs were formed in a disposable cuvette, and the size measurement was conducted immediately. For aqueous media and moderate electrolyte concentration, the Smoluchowski approximation is suitable for

the PEC. The zeta potential was calculated by the Henry equation after measurement of the electrophoretic mobility. In the zeta potential measurements, disposable capillary cells (DTS1070) were used. After PECs were formed, the mixture was transferred to the capillary cell to carry out the zeta potential measurements.

2.5 Simulations of PECs

Classical molecular dynamics simulations in all-atom detail were performed to investigate the effective charge distribution around the complexes with and without excess salt with the motivation that electrostatic barriers dominate the colloidal stability of the PEC solution. COMPASS (Condensed-Phase Optimized Molecular Potentials for Atomistic Simulation Studies) force field, and its explicit 3-site fully flexible water model[57] within Accelrys Materials Studio software[57, 58] were used. The force field and its water model have been validated extensively for conformational and solubility properties of polymers.[59, 60] The simulations are performed in the NPT ensemble using Andersen barostat,[61] Nosé-Hoover-Langevin thermostat,[62-66] and Ewald summation with accelerated convergence of lattice sums[67, 68] for long range electrostatics.

The PDAC/PSS complexes were modeled in compositions of 5 PSS_{40} - 1 $PDAC_{40}$, 3 PSS_{40} – 3 $PDAC_{40}$, and 1 PSS_{40} – 5 $PDAC_{40}$ chains (corresponding to experimental mol% PDAC molar fractions of 17, 50, and 83). The subscript 40 refers to the length of each polyelectrolyte chain in repeat units in the simulations. For each composition, three salt concentrations matching the experimental range were considered: no added salt (just the native counterions), 1 M excess NaCl, and 2 M excess NaCl as ions. For each composition and salt concentration, 1.1 ns simulations using three different initial configurations were run. Simulation box size is between $(7.8\ nm)^3$ and $(8.1\ nm)^3$ depending on the system resulting in density of 1.07-1.11 g/cm^3. The complex structure and the cumulative charge (charge contained within that distance) distribution were analyzed.[69, 70] Further simulation setup details and configuration preparation are provided as ESI.

3. Results

3.1 Visual inspection of PECs with time

There are a number of ways to create PECs, which brings difficulty in comparing across studies. PECs tend to exist in kinetically trapped, path-dependent states[8] in which even the order of polyelectrolyte addition affects properties (Figure S1). For this reason, we arbitrarily chose to always mix PDAC into PSS so as to solely focus on ionic strength and mixing ratio effects. The total concentration of the PDAC and PSS repeat units was kept constant at 10 mM. The NaCl concentration was varied from 0 to 3 M, and the mole percentage of PDAC repeat units was varied from 20 to 80 mol% (relative to the total concentration of PDAC and PSS repeat units). In all cases, the solution became turbid upon mixing, consistent with the formation of PECs. The resulting PECs were classified into “stable”, “unstable”, or “solution” states, as defined below.

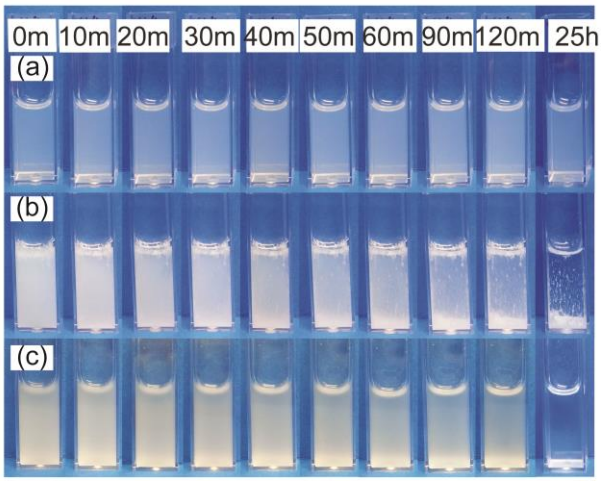

Fig. 1 Time-lapsed digital images of PECs formed by mixing PDAC and PSS: (a) 20 mol% PDAC, 0.5 M NaCl “stable” PECs and (b) 50 mol% PDAC, 0.5 M NaCl “unstable” PECs and (c) 50 mol% PDAC, 3.0 M NaCl PECs that dissolve. Total concentration of PDAC and PSS repeat units (10 mM) were identical for all cases. Concentrations are on a repeat unit basis.

Figure 1a shows an example of stable PECs (20 mol% PDAC, 0.5 M NaCl). Upon mixing (0 min) the stable PECs generally had lower turbidity as compared to the unstable PECs. The mixture was left undisturbed and observed over the course of seven days, with no visible changes in appearance. For those mixtures whose turbidity or overall appearance remained constant, we assign them as “stable”. Stable PECs were generally observed for highly nonstoichiometric mixing ratios (20 or 80% mol% PDAC) and low ionic strength, with exceptions noted later. Centrifugation of the stable PECs yielded a precipitate at the bottom of the vial, having an irregular structure (Figure S2 and S3), which is consistent with a complex solid phase rather than a complex coacervate phase.

Figure 1b shows an example of “unstable” PECs (50 mol% PDAC, 0.5 M NaCl). Initially, the mixture was very turbid, followed by a gradual decrease in turbidity while a white string-like precipitate formed. The white precipitate either fell to the bottom or adhered to the walls of the cuvette. Again, the mixture was undisturbed over this time, with no centrifugation. Unstable PECs were generally observed when PDAC and PSS were mixed at or near 1:1 stoichiometry, or with high ionic strength.

Figure 1c shows an example of PECs (50 mol% PDAC, 3.0 M NaCl) that quickly form but then dissolve gradually over the course of time. Initially, the complex was turbid, indicating the formation of complex. In contrast to Figure 1b, the turbidity decreased gradually with time without any precipitate formation. At 25h after preparation, the complex was totally clear. This behaviour was generally observed at high ionic strengths (2.5 – 3.0 M NaCl). Almost a day after mixing, centrifugation resulted in a single phase, and optical microscopy similarly showed no evidence of complex precipitate or complex coacervate formation, thus suggesting the presence of a

solution phase. It is possible that a small fraction of coacervate phase exists such that it is not observable by these means. For simplicity, we discuss this phase as a solution.

3.2 Turbidity measurements

From our initial screening, it is clear that the ratio of PDAC to PSS repeat units and the ionic strength of the solution both play large roles in the stability of the resultant PECs. Turbidity measurements, popularly employed to investigate the properties of PECs,[24, 28] were performed on PEC mixtures both newly prepared and aged for seven days without disturbance.

Figure 2a shows a turbidity map of newly prepared PECs as a function of composition and salt concentration. In terms of composition, the turbidity was lowest at highly nonstoichiometric PDAC/PSS ratios (20 or 80 mol% PDAC). As for salt, the turbidity was lowest when the NaCl concentration was low or equal to zero. As an exception, the turbidity was particularly high for the 50 mol% PDAC PEC, even in the absence of salt. After seven days, the turbidity contour map was very different, Figure 2b. It is first interesting to note that most of the contour map indicates a very low level of turbidity, and the color scale for turbidity decreases from 5.2 to 1.3 a.u for PECs aged seven days vs. those freshly prepared. Instead, it is indicative of the formation white solid precipitate, falling to the bottom of the cuvette and leaving behind a transparent, polymer-deficient phase, Figure 1b. At higher salt concentrations, this drop in turbidity is commensurate with the dissolution of PECs, Figure 1c. On the other hand, only at low NaCl concentrations and nonstoichiometric PDAC/PSS ratios did turbidity remain, consistent with the stable complexes shown in Figure 1a.

From Figure 2, it is possible to discern the colloidally stable/unstable PEC boundary as the condition at which turbidity does or does not change over the course seven days. However, it should be noted that turbidity alone is not sufficient to demarcate between complexes that dissolve at high salt concentrations and those that are colloidally unstable at intermediate salt concentrations. The general shape of the stable/unstable PEC boundary bottoms out 50 mol% PDAC and 0.2 M NaCl. At 50 mol% PDAC and intermediate NaCl concentrations, PEC precipitation was observed. On the other hand, for 20 mol% PDAC, the salt concentration for PEC precipitation was much higher at 1.5 M. The boundary appears mostly symmetric with only slight skewing.

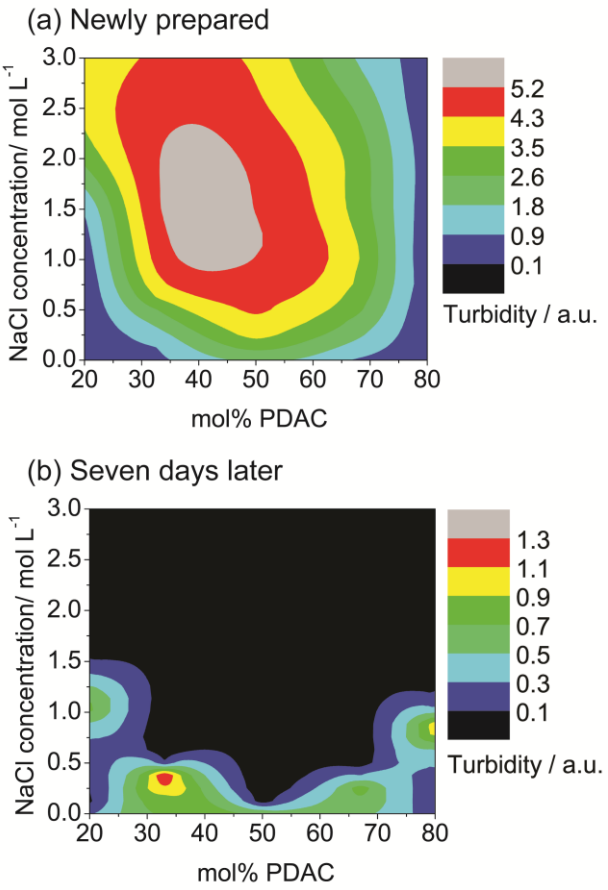

Fig.2 Turbidity of PEC mixtures: (a) newly prepared PECs and (b) aged seven days without disturbance. Turbidity was measured using UV-Vis-NIR spectroscopy and calculated as described in the Materials and Methods section.

To further capture the evolution of turbidity with respect to time, the turbidity of newly formed complexes of each type (unstable, stable, and dissolving) were monitored over the course of 25 h, Figure 3. For the dissolving PEC (50 mol% PDAC, 3 M NaCl) the turbidity was initially high at the beginning, but decreased slowly with time. This turbidity change is consistent with the initial formation of a complex and its gradual dissolution into solvated polyelectrolyte chains. The unstable PEC (XXX mol% PDAC, XXX M NaCl) exhibited similar behaviour, except that the loss of turbidity arises from the precipitation of PECs. The stable PECs (XXX mol% PDAC, XXX M NaCl) exhibited no change in turbidity, consistent with visual observation.

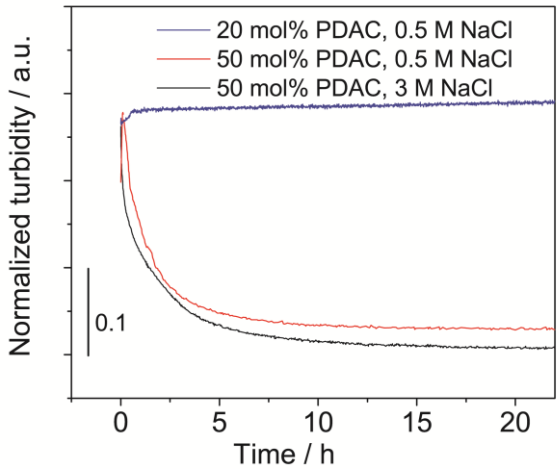

Fig.3 Turbidity of newly prepared stable, unstable, and dissolving PECs (20 mol% PDAC and 0.5 M NaCl, 50 mol% PDAC and 0.5 M NaCl, and 50 mol% PDAC and 3 M NaCl, respectively). Each curve was shifted vertically on the y-axis to have the same initial turbidity.

3.3 Hydrodynamic size and zeta potential measurements

To probe the origin of PEC stability, dynamic light scattering was employed to measure the temporal dependence of the PECs' hydrodynamic diameters, Figure 4. We have found that a nine-minute observation window is sufficient for identifying stable vs. unstable PECs even though large-scale precipitation tends to occur over the course of days. Because dissolution of complexes at high salt concentrations occurs over the course of hours, this approach is not reliable in distinguishing between unstable PECs and dissolving PECs. Over a longer time scale, unstable PECs aggregated together such that their size and dispersity became so large that DLS was no longer reliable. However for stable PECs, the hydrodynamic size remained constant over the course of 25 hours, Figure S3. We have denoted the data for which the polydispersity is greater than 0.7 by the shading in Figure 4. The shaded data loosely coincides with unstable and dissolving PECs, although there are some unstable PECs for which the polydispersity was below the 0.7 cutoff.

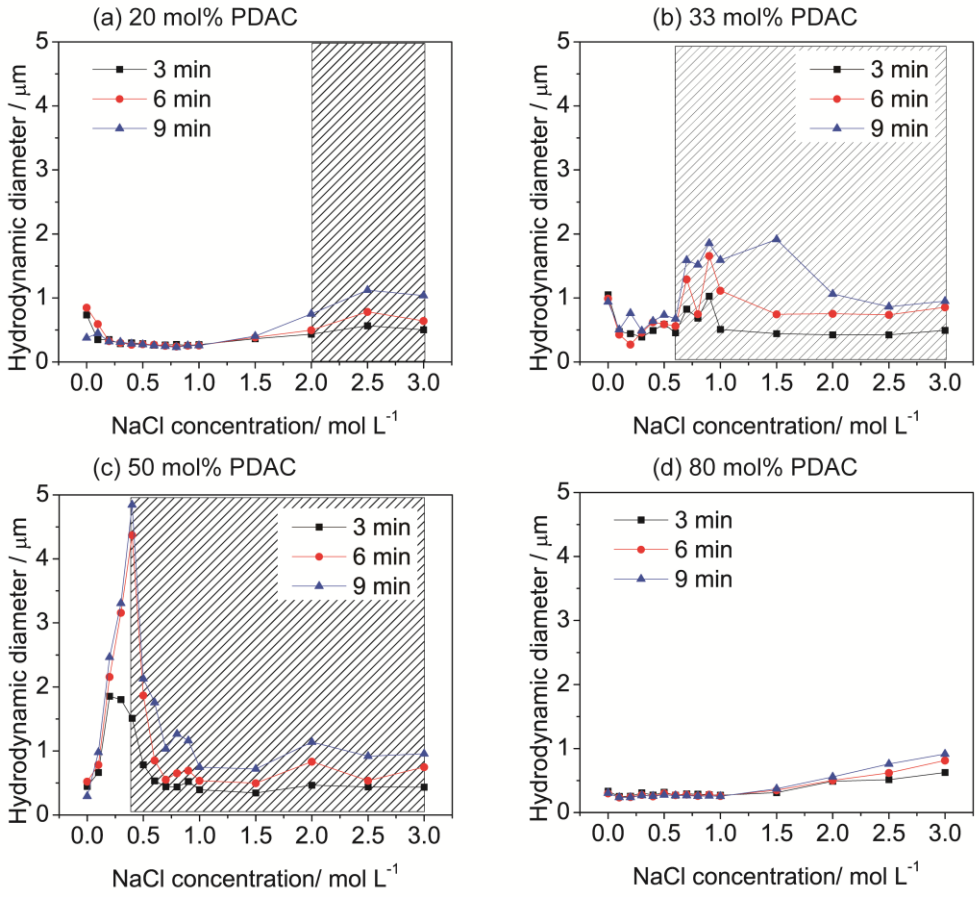

Fig.4 Hydrodynamic diameters of PECs with varying compositions measured using DLS. The shaded region denotes data in which the polydispersity was > 0.7, so the exact hydrodynamic diameter is uncertain

For highly nonstoichiometric PECs (20 and 80 mol% PDAC), the boundary between stable and unstable is quite clear, Figure 4a and 4d. Below 1.5 M NaCl, PEC hydrodynamic size (230 nm to 320 nm) remained constant over the course of nine minutes, consistent with stable PECs. Above a NaCl concentration of 1.5 M, the hydrodynamic diameter steadily increased with time, consistent with unstable PECs. Therefore, the critical salt concentration for colloidal stability at these highly

nonstoichiometric conditions can be assigned to 1.5 M NaCl. These results match well with the boundaries defined by UV-Vis-NIR turbidity measurements presented earlier.

For a stoichiometric composition (50 mol% PDAC, Figure 4c), PEC hydrodynamic diameter increased regardless of NaCl concentration, suggestive of instability. PEC size was particularly large, on the order of microns, when NaCl concentrations were between 0.2 mol/L to 0.5 mol/L. These results mirror the very turbid region, for which larger particles are more effective light scatters, depicted in Figure 2a for freshly prepared complexes.

Zeta potential is another convenient means to probe the origin of PEC stability. It has been posited by Li and coworkers that zeta potentials above |30 mV| yield stable colloidal suspensions and that those below are marginal or unstable.[72, 73] Figure 5 shows average zeta potentials of three separate measurements for PEC mixtures as a function of ionic strength and mixing ratio. It is acknowledged that experimental error is introduced when highly aggregating systems are examined by zeta potential. Therefore, to reduce this effect, we examined only freshly prepared PECs. For PECs prepared from 50 mol% PDAC and above, the zeta potentials were positive. In contrast, the zeta potentials were negative for PECs prepared from 33 mol% PDAC and below. As the ionic strength increased, the zeta potentials approached zero. At a given NaCl concentration, the absolute zeta potential of the stoichiometric PEC was lowest. When PSS was in excess, the zeta potential was larger in magnitude as compared to the case when PDAC is in excess. This is due to the hydrophilicity differences between PDAC and PSS, which is consistent with previous work where the more hydrophilic excess polyelectrolyte showed lower zeta potentials.[74] It is also curious that a stoichiometric complex should exhibit a positive zeta potential, whereas a value of zero might be expected; this result is possibly attributed to differences in PDAC and PSS hydrophilicity as well. Applying the criteria put forth by Li and coworkers, the zeta potential of |30 mV| occurred at a NaCl concentration of about 1.5 mol/L for 20 mol% PDAC, for example.

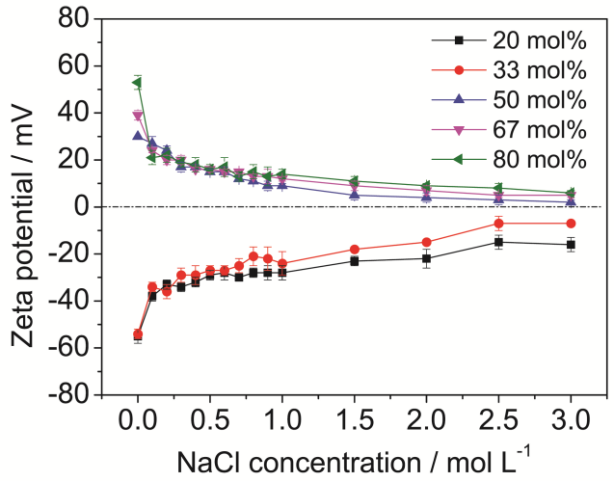

Fig.5 Zeta potential of newly prepared PDAC/PSS PECs. The composition is given in mol% PDAC.

3.4 Molecular simulations of PECs

All-atom molecular dynamics simulations were performed to characterize the structure of the PECs with the aim of using the structural insight gained to connect the experimentally observed behavior with its molecular origins. Figure 6 shows examples for the final structures of PECs simulated at varying molar ratios without any additional salt. The Na^+ and Cl^- ions shown are counterions arising from the original polyelectrolyte prior to complexation. The 1 ns simulational relaxation performed on the PECs was sufficient for ion distribution equilibration but not for major structural reorganization of the complex. This means that the individual simulations represent kinetically trapped configurations – even though the data presented throughout is an average of different initial configurations, the electrostatic barriers obtained in this fashion are estimates and their magnitudes rely directly on the PEC dimensions (choice of simulation system size). Furthermore, no evaluation of the difference in steric barriers between excess PDAC and PSS was considered here as the charging was assumed to dictate behavior. We emphasize that the simulational charge distributions reflect only qualitatively the stability of the complexes. While the polymer ratios match, the size of the complexes in experiments and in the simulations differs significantly because of different polymer lengths. As a result, the simulated complexes represent in small form the resulting charge distribution from that particular mixing ratio. In these simulations, the polyelectrolyte component in excess wraps around the minority component to form the complex. This results in the excess component dictating the outward characteristics of the PEC. It is noted that the excess component may remain partially soluble in the aqueous phase.

The temporal stability of PECs is dictated by the barriers in their free energy landscape needed to deter aggregation. For charged molecular aggregates, these barriers typically arise dominantly from charge repulsion although polymeric components have significant steric barriers as well. To get insight towards the barrier, we calculated the effective charge distribution for the PECs formed at 17, 50 and 83 mol% PDAC in the presence of no added salt, 1 M, and 2 M excess NaCl (Figure 7). First, the data show that all PECs are effectively neutral near their core but that the PECs formed in excess of one component have significant effective charging at distances corresponding to their surface (at distances between 2.5 nm-4.5 nm from the center of mass of the simulated PECs). This charging was stronger for excess PSS than for excess PDAC because as the more hydrophilic of the two, PDAC packs more loosely on the PEC surface in the simulations. As a consequence, in the experiments, a molar ratio corresponding to excess PSS results in a higher zeta potential value than the reverse excess PDAC case. These results support the experimentally observed asymmetry in the temporal stability and PEC size distribution. Specifically, the excess charge from PDAC is distributed over a larger space than with a corresponding amount of excess PSS. For the stoichiometric composition, some local charging at the PEC surface was observed in the simulations but was neutral overall.

The effect of NaCl was particularly pronounced in the snapshots and the cumulative charge distribution. As NaCl concentration increased from 1 M and 2 M, the effective charge at distances between 2.5 nm-4.5 nm became screened for the nonstoichiometric compositions. A concentration of 2 M NaCl resulted in a relatively flat charge distribution in the simulational PECs. Specifically, in the presence of excess salt, screening resulted dominantly from ions condensing to the outer PEC surface and partially from ions entering the PEC itself. For the case of no added salt, the solvated counterions entered the complex for nonstoichiometric compositions (contributing to charge neutralization in the core), whereas counterions tended to remain outside the complex for stoichiometric composition (with the core being compensated intrinsically by the polyelectrolytes themselves).

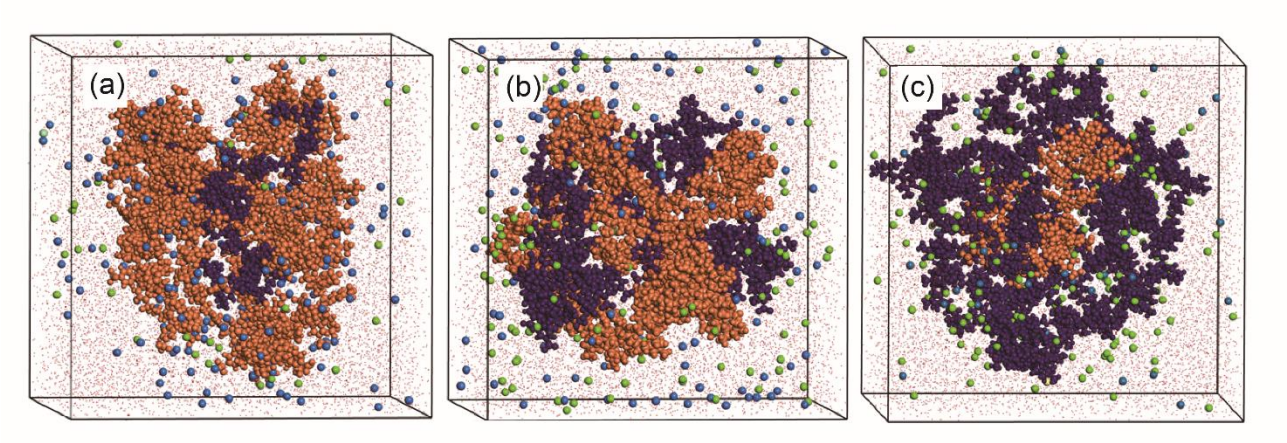

Fig.6 Representative snapshots of PDAC/PSS complexes with (a) 17, (b) 50, and (c) 83 mol% PDAC (5 PSS_{40}-1 $PDAC_{40}$, 3 PSS_{40}-3 $PDAC_{40}$, and 1PSS_{40}-5 $PDAC_{40}$ systems, see Materials and Methods for details). PSS is highlighted in orange, PDAC in dark blue, Na^+ ions in purple, and Cl^- in green.

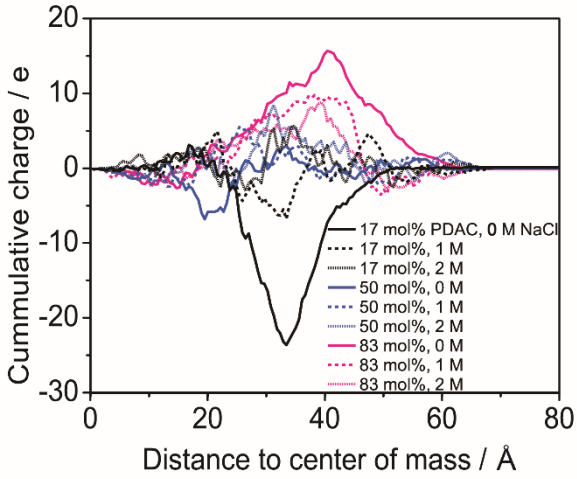

Fig.7 Effective charge distribution calculated for PDAC/PSS complexes of varying composition (17, 50, and 83 mol% PDAC) and salt concentration (0, 1, and 2 M added NaCl). Each data curve measures the cumulative charge resulting from the presence of PSS, PDAC, and any ions in the solution as a function of distance from the center of mass of the PEC.

4. Discussion

The process of complexation is governed by a two-step mechanism: formation of primary PEC particles, followed by growth of secondary PECs from the aggregation of the primary particles.[26, 75] The appearance of white string-like precipitates in our unstable PDAC/PSS complex is consistent with the formation of secondary PEC aggregates. On the other hand, stable PDAC/PSS complexes appear to consist of mostly primary particles, as evidenced by the lack of change in hydrodynamic diameter with time. We will first begin our discussion of stability by addressing the effects of salt and composition, which appear to strongly control the time-dependent behavior of PECs.

Without added salt, all PECs exhibited stable behavior. The mixtures remained turbid over seven days, and the hydrodynamic diameter did not change appreciably. The hydrodynamic diameters were in the range of 230 to 320 nm and the zeta potentials were greater than |30 mV| for all compositions. It is noted that some compositions exhibited a second population of larger particles, which we believe are secondary particles. However, the lack of change in the diameter and turbidity with time suggests that further particle aggregation and growth was arrested. Given the high absolute zeta potential and the charge density profiles from simulations, it is likely that aggregation and growth of secondary particles is arrested by electrostatic interactions and self-repulsion of PECs.

In the presence of added NaCl, screening occurs, which is characterized by a drop in absolute zeta potential and instability of PECs. Simulations support this idea, and also shed light on the location of small counterions. As salt concentration increases, there is a marked shift of counterions condensed at the PEC surface to counterions present throughout the PEC. These results, in the broader context, support observations of "saloplastics" by the Schlenoff group, who have also observed the influence of salt.[36-41, 49, 51] At even higher salt concentrations (< 2.5 M NaCl), the screening effect is strong and electrostatic interactions, which hold the polyelectrolyte chains together, are

weakened.[30] This is readily observed by the behaviour in Figure 1c, where a complex is initially formed, but then gradually dissolves.

We next turn to the effect of composition on stability, hydrodynamic diameter, and zeta potential. Inspection of Figure 2 shows that PECs formed at stoichiometric compositions were initially very turbid; after seven days, the solution became transparent as much of the PEC has precipitated or dissolved, depending on salt concentration. This result is explained by the zeta potential of the stoichiometric composition, which is generally lower in absolute value as compared to the highly nonstoichiometric cases. Simulations support this idea, in which the charge distribution of stoichiometric complexes shows only a small amount of cumulative charge regardless of salt concentration. Experimentally, the stoichiometric complex formed at 0.2 M NaCl (zeta potential of +23.6 mV) lies at the transition from being colloidally stable to unstable. The weak charging on stoichiometric PECs is hence the primary reason that they are more susceptible to aggregation and eventual precipitation as compared to the nonstoichiometric case. It is possible that the weak charging on the PECs is associated with the penetration of unassociated salt into the complex.

For the case of nonstoichiometric compositions (20 and 80 mol% PDAC), the behavior is markedly different. Much higher salt concentrations (1.5 M NaCl) were required to render the PECs unstable. For example, the hydrodynamic diameter remained around 230 nm to 320 nm for nonstoichiometric PECs at salt concentrations below 1.5 M NaCl; in comparison, stoichiometric complexes were generally much larger as they were comprised of growing secondary PECs. These results are consistent with zeta potential measurements, in which the absolute zeta potential is highest for the most nonstoichiometric compositions. Simulations also support that nonstoichiometric PECs have a highly charged surface. Therefore, we conclude that the zeta potential of the PEC (which is affected by composition and salt concentration) is primarily responsible for the observed stability trends.

The composition dependence on turbidity is noteworthy. The contour map shown in Figure 2a is somewhat symmetric with slight skewing towards the left. One might expect such a contour map to be symmetric, but the result here is otherwise. One potential reason for this result is that PSS is more hydrophobic than PDAC, thus driving phase separation and increased turbidity at higher PSS compositions. Another possible reason is ascribed to differences in polymer structure or chain flexibility.[20] Else, the mismatch in the linear charge density between PDAC and PSS might explain the slight skewing; PDAC has one charge per four carbons on its backbone, whereas PSS has one charge per two carbons.

Considering simulation and experimental results, the skewing is most likely a result of differences in hydrophilicity between the two polymers. Considering two cases where the compositions are nonstoichiometric but PDAC -PSS ratios are reversed (20 mol% PDAC vs. 80 mol% PDAC), the 20 mol% PDAC complexes generally had higher absolute zeta potential as compared to the reverse case with 80 mol% PDAC PECs. Our simulations have shown that PDAC is more hydrophilic than PSS, and that when excess PDAC is part of the PEC, the PDAC shell is much more diffuse and PDAC samples more of the solution space as opposed to the reverse case. This result possibly yields a lower apparent zeta potential for the case of excess PDAC.

From these results, we propose a diagram the colloidally stable/unstable and colloidally unstable/solution boundaries, Figure 8. The lower orange curve demarcates the boundary between colloidally stable (region a) and unstable (region b) states; the upper brown striped curve separates the colloidally unstable and solution (region c) states). The a-b boundary was selected as the salt concentration at which a steady change in hydrodynamic diameter with time emerges, Figure 4. We chose to assign the a-b boundary in this manner as the temporal evolution of hydrodynamic diameter matches well with the turbidity diagram shown in Figure 2. The b-c boundary was chosen from long-term visual inspection of PDAC-PSS mixtures, since DLS and turbidity were unsuitable. The curve is not drawn to be sharp – rather there exists a transition zone where intermediate behaviour was sometimes observed.

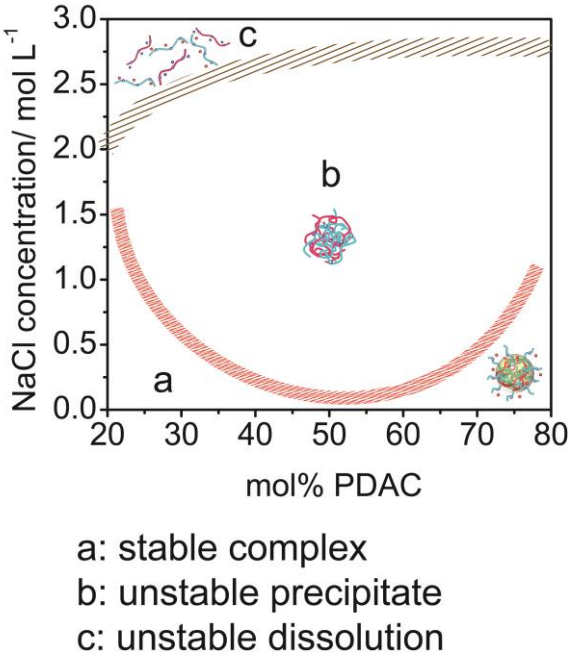

Fig. 8 Diagram of PDAC-PSS behaviour as a function of salt concentration and PDAC content. Regions *a*, *b*, and *c* stand for PECs that are colloidally stable, unstable, or dissolving, respectively. The insets depict possible PEC configurations that lend themselves towards specific phase behaviour.

The origin of stability and instability arises from the mechanism of PEC formation. Let us consider the nonstoichiometric composition with no added salt as an example of the stable case. Upon initial mixing of the two polyelectrolytes, neutral small-size primary PEC particles are formed, and then excess polyelectrolyte surrounds the PEC particle nucleus. The formation of PECs with neutral cores and stabilization from the excess polyelectrolyte has previously been reported by Dautzenberg et al.[8] Our findings are in full agreement, where the initial state is typified by PEC particles of high absolute zeta

potential (> 30 mV) and size of about 200-400 nm. The charge on the primary PECs is sufficiently large so as to illicit self-repulsion and long-term stability, rather than aggregation and precipitation.[26] However, as the ionic strength increases, small counterions screen and penetrate the PECs, the zeta potential decreases, and the PECs aggregate, resulting in larger secondary PECs and eventual precipitation.[76] At even higher concentrations, ion-pairing is screened and PECs, if initially formed, dissolve into soluble chains. This mechanism has also been reported computationally[70] . The drawings inside Figure 8 depict the observed states.

Our molecular simulations aid in pinpointing the origins of stability: PECs assembled at uneven molar ratios in low ionic strength possess a charge-charge repulsion which acts as a barrier against their aggregation when the PECs diffuse to distances corresponding to the peak in cumulative charge. Excess PSS results in enhanced effective charge, and therefore higher adsorption barrier, in comparison to PDAC in the simulations. This is because PDAC extends further to the aqueous phase due to its more hydrophilic nature; the position, form, and height of the PEC cumulative charge peak depends naturally on the polyelectrolytes and on the size of the complex. Experimentally, this manifests as slight asymmetry in the temporal stability and aggregate size development between different excess PSS and excess PDAC ratios (excess PDAC results in temporally more stable PECs). At stoichiometric composition, the effective PEC charge, and the repulsion resulting from it is significantly smaller, and correspondingly, the stability is reduced. Excess salt results in screening of the charge peak and similar outcome. Hence, decreased temporal stability, and enhanced aggregation propensity is expected for stoichiometric compositions and/or high assembly solution ionic strength, as shown by the experimental data.

5. Conclusions

In this work, we outlined the conditions (ionic strength and polycation/polyanion composition) that form the boundary between colloidally stable and unstable polyelectrolyte complexes, as well as solutions. This was accomplished by monitoring PEC turbidity and hydrodynamic diameter as a function of time, and by comparing the zeta potential of PECs against experimental simulations. Stable PECs were typified by a constant turbidity and hydrodynamic diameter with respect to time, and were most commonly observed for conditions of no added salt and/or nonstoichiometric composition. Further, stable PECs exhibited a high absolute zeta potential and a cumulative charge focused at the PEC corona or shell. On the other hand, unstable PECs exhibit a gradual formation of a string-like precipitate and a steady increase in hydrodynamic diameter with time, and were most commonly observed at high ionic strength and/or stoichiometric composition. The absolute zeta potential of unstable PECs was low, and the cumulative charge profile was near-flat, consistent with the formation of a neutral particle. It is the action of these neutral particles, aggregating into larger secondary particles, that leads to colloidal instability and the formation of precipitate. Aggregation, colloidal stability, and dissolution appear to be controlled by a complex interplay of screening by added salt within the PEC particle.

These results represent only an early step in understanding the temporal behavior of PECs, which tend to exist in a metastable or kinetically trapped state. Future work should focus upon other polyelectrolytes families (i.e., weak polycations and polyanions), pH conditions, and temperatures. Here, we investigated only strong polyelectrolytes, which are not very responsive to pH. Future studies with weak polyelectrolytes and pH with respect to time should provide a rich area of study. Varying temperature may also prove interesting, in which temperature provides a potential handle to move the stable/unstable boundary or to accelerate the rate of PEC aggregation.

Acknowledgements

This work was supported in part by the National Science Foundation Grant No. 1312676 (J.L.), Academy of Finland (E.Y., H.A., M.S.), and Marie Curie Career Integration Grants within the 7th European Community Framework Programme through Grant 293861 (M.S.). The computational results of this research have been achieved using the PRACE Research Infrastructure resources based in Finland at CSC–IT Center for Science and the CSC – IT Center for Science, Finland national resources. We thank Dr. Mustafa Akbulut of Texas A&M University for Zetasizer Nano, ZS90 and Dr Carrie Schindler of Malvern for assistance with DLS analysis and the TAMU Materials Characterization Facility.

References

1 1. A. S. Michaels, *Industrial & Engineering Chemistry*, 1965, **57**, 32-40.
2 2. Y. Li, B. S. Lokitz and C. L. McCormick, *Angewandte Chemie International Edition*, 2006, **45**, 5792-5795.
3 3. M. Yin, B. Gu, Q. Zhao, J. Qian, A. Zhang, Q. An and S. He, *Anal Bioanal Chem*, 2011, **399**, 3623-3631.
4 4. D. Priftis, R. Farina and M. Tirrell, *Langmuir*, 2012, **28**, 8721-8729.
5 5. X.-S. Wang, Q.-F. An, F.-Y. Zhao, Q. Zhao, K.-R. Lee, J.-W. Qian and C.-J. Gao, *Cellulose*, 2014, **21**, 3597-3611.
6 6. Z. Lin, J. Chang, J. Zhang, C. Jiang, J. Wu and C. Zhu, *Journal of Materials Chemistry A*, 2014, **2**, 7788-7794.
7 7. Y. JeongáOh, I. HwanáCho and S. YoungáPark, *Chemical Communications*, 2012, **48**, 11895-11897.
8 8. H. Dautzenberg and W. Jaeger, *Macromolecular Chemistry and Physics*, 2002, **203**, 2095-2102.
9 9. B. Philipp, H. Dautzenberg, K.-J. Linow, J. Kötz and W. Dawydoff, *Progress in Polymer Science*, 1989, **14**, 91-172.
10 10. A. Veis, *The Journal of Physical Chemistry*, 1963, **67**, 1960-1964.
11 11. E. Tsuchida, Y. Osada and K. Abe, *Die Makromolekulare Chemie*, 1974, **175**, 583-592.

12 12. V. A. Kabanov and A. B. Zezin, *Pure and Applied Chemistry*, 1984, **56**, 343-354.
13 13. M. A. C. Stuart, N. A. M. Besseling and R. G. Fokkink, *Langmuir*, 1998, **14**, 6846-6849.
14 14. C. B. Bucur, Z. Sui and J. B. Schlenoff, *Journal of the American Chemical Society*, 2006, **128**, 13690-13691.
15 15. D. Priftis, N. Laugel and M. Tirrell, *Langmuir*, 2012, **28**, 15947-15957.
16 16. E. Tsuchida, Y. Osada and K. Sanada, *Journal of Polymer Science Part A-1: Polymer Chemistry*, 1972, **10**, 3397-3404.
17 17. S. L. Perry, L. Leon, K. Q. Hoffmann, M. J. Kade, D. Priftis, K. A. Black, D. Wong, R. A. Klein, C. F. Pierce Iii, K. O. Margossian, J. K. Whitmer, J. Qin, J. J. de Pablo and M. Tirrell, *Nat Commun*, 2015, **6**.
18 18. A. S. Michaels and R. G. Miekka, *The Journal of Physical Chemistry*, 1961, **65**, 1765-1773.
19 19. J. Požar and D. Kovačević, *Soft matter*, 2014, **10**, 6530-6545.
20 20. H. Sato and A. Nakajima, *Polym J*, 1975, **7**, 241-247.
21 21. N. P. Birch and J. D. Schiffman, *Langmuir*, 2014, **30**, 3441-3447.
22 22. S. Lim, D. Moon, H. J. Kim, J. H. Seo, I. S. Kang and H. J. Cha, *Langmuir*, 2014, **30**, 1108-1115.
23 23. C. Márquez-Beltrán, L. Castañeda, M. Enciso-Aguilar, G. Paredes-Quijada, H. Acuña-Campa, A. Maldonado-Arce and J.-F. Argillier, *Colloid and Polymer Science*, 2013, **291**, 683-690.
24 24. D. Priftis and M. Tirrell, *Soft Matter*, 2012, **8**, 9396-9405.
25 25. R. Chollakup, W. Smitthipong, C. D. Eisenbach and M. Tirrell, *Macromolecules*, 2010, **43**, 2518-2528.
26 26. V. Starchenko, M. Müller and N. Lebovka, *The Journal of Physical Chemistry B*, 2012, **116**, 14961-14967.
27 27. H. Dautzenberg and N. Karibyants, *Macromolecular Chemistry and Physics*, 1999, **200**, 118-125.
28 28. D. Priftis, X. Xia, K. O. Margossian, S. L. Perry, L. Leon, J. Qin, J. J. de Pablo and M. Tirrell, *Macromolecules*, 2014, **47**, 3076-3085.
29 29. N. Lebovka, in *Polyelectrolyte Complexes in the Dispersed and Solid State I*, ed. M. Müller, Springer Berlin Heidelberg, 2014, vol. 255, ch. 171, pp. 57-96.
30 30. Q. Wang and J. B. Schlenoff, *Macromolecules*, 2014, **47**, 3108-3116.
31 31. A. B. Zezin and V. A. Kabanov, *Russian Chemical Reviews*, 1982, **51**, 833-855.
32 32. S. A. Sukhishvili, E. Kharlampieva and V. Izumrudov, *Macromolecules*, 2006, **39**, 8873-8881.
33 33. N. Laugel, C. Betscha, M. Winterhalter, J.-C. Voegel, P. Schaaf and V. Ball, *The Journal of Physical Chemistry B*, 2006, **110**, 19443-19449.
34 34. A. Salehi, P. S. Desai, J. Li, C. A. Steele and R. G. Larson, *Macromolecules*, 2015, **48**, 400–409.
35 35. V. Izumrudov, E. Kharlampieva and S. A. Sukhishvili, *Macromolecules*, 2004, **37**, 8400-8406.
36 36. R. F. Shamoun, A. Reisch and J. B. Schlenoff, *Advanced Functional Materials*, 2012, **22**, 1923-1931.
37 37. R. A. Ghostine, R. F. Shamoun and J. B. Schlenoff, *Macromolecules*, 2013, **46**, 4089-4094.
38 38. R. F. Shamoun, H. H. Hariri, R. A. Ghostine and J. B. Schlenoff, *Macromolecules*, 2012, **45**, 9759-9767.
39 39. C. H. Porcel and J. B. Schlenoff, *Biomacromolecules*, 2009, **10**, 2968-2975.
40 40. P. Tirado, A. Reisch, E. Roger, F. Boulmedais, L. Jierry, P. Lavalle, J. C. Voegel, P. Schaaf, J. B. Schlenoff and B. Frisch, *Advanced Functional Materials*, 2013, **23**, 4785-4792.
41 41. A. Reisch, E. Roger, T. Phoeung, C. Antheaume, C. Orthlieb, F. Boulmedais, P. Lavalle, J. B. Schlenoff, B. Frisch and P. Schaaf, *Advanced Materials*, 2014, **26**, 2547-2551.
42 42. B. Qiao, J. J. Cerdà and C. Holm, *Macromolecules*, 2010, **43**, 7828-7838.
43 43. H. Dautzenberg, *Macromolecules*, 1997, **30**, 7810-7815.
44 44. H. Dautzenberg, *SURFACTANT SCIENCE SERIES*, 2001, 743-792.
45 45. H. Dautzenberg and G. Rother, *Macromolecular Chemistry and Physics*, 2004, **205**, 114-121.
46 46. N. Karibyants and H. Dautzenberg, *Langmuir*, 1998, **14**, 4427-4434.
47 47. N. Karibyants, H. Dautzenberg and H. Coelfen, *Macromolecules*, 1997, **30**, 7803-7809.
48 48. H. H. Hariri, A. M. Lehaf and J. B. Schlenoff, *Macromolecules*, 2012, **45**, 9364-9372.
49 49. H. H. Hariri and J. B. Schlenoff, *Macromolecules*, 2010, **43**, 8656-8663.
50 50. J. A. Jaber and J. B. Schlenoff, *Journal of the American Chemical Society*, 2006, **128**, 2940-2947.
51 51. M. Z. Markarian, H. H. Hariri, A. Reisch, V. S. Urban and J. B. Schlenoff, *Macromolecules*, 2011, **45**, 1016-1024.
52 52. U. Böhme and U. Scheler, *The Journal of Physical Chemistry B*, 2007, **111**, 8348-8350.
53 53. B. Fortier-McGill and L. Reven, *Macromolecules*, 2008, **42**, 247-254.
54 54. W. Ouyang and M. Müller, *Macromolecular bioscience*, 2006, **6**, 929-941.
55 55. Á. W. Imre, M. Schönhoff and C. Cramer, *The Journal of chemical physics*, 2008, **128**, 134905.
56 56. S. L. Perry, Y. Li, D. Priftis, L. Leon and M. Tirrell, *Polymers*, 2014, **6**, 1756-1772.
57 57. H. Sun, *The Journal of Physical Chemistry B*, 1998, **102**, 7338-7364.
58 58. *Material Studio Modeling Environment*, Accelrys Software Inc., San Diego, Calif, USA, 2011.
59 59. T. Spyriouni and C. Vergelati, *Macromolecules*, 2001, **34**, 5306-5316.
60 60. H. Sun and D. Rigby, *Spectrochimica Acta Part A: Molecular and Biomolecular Spectroscopy*, 1997, **53**, 1301-1323.
61 61. H. C. Andersen, *The Journal of chemical physics*, 1980, **72**, 2384-2393.
62 62. B. Leimkuhler, E. Noorizadeh and F. Theil, *Journal of Statistical Physics*, 2009, **135**, 261-277.

63 63. A. A. Samoletov, C. P. Dettmann and M. A. Chaplain, *Journal of Statistical Physics*, 2007, **128**, 1321-1336.
64 64. P. H. Hünenberger, in *Advanced Computer Simulation*, eds. C. Dr. Holm and K. Prof. Dr. Kremer, Springer Berlin Heidelberg, 2005, vol. 173, ch. 2, pp. 105-149.
65 65. B. Leimkuhler, E. Noorizadeh and O. Penrose, *Journal of Statistical Physics*, 2011, **143**, 921-942.
66 66. N. Shuichi, *Progress of Theoretical Physics Supplement*, 1991, **103**, 1-46.
67 67. P. Ewald, *Ann. Phys*, 1921, **64**, ll.
68 68. N. Karasawa and W. A. Goddard III, *The Journal of Physical Chemistry*, 1989, **93**, 7320-7327.
69 69. H. S. Antila, M. Harkonen and M. Sammalkorpi, *Physical Chemistry Chemical Physics*, 2015, **17**, 5279-5289.
70 70. H. S. Antila and M. Sammalkorpi, *The Journal of Physical Chemistry B*, 2014, **118**, 3226-3234.
71 71. J. Chen, J. A. Heitmann and M. A. Hubbe, *Colloids and Surfaces A: Physicochemical and Engineering Aspects*, 2003, **223**, 215-230.
72 72. D. Li, M. B. Muller, S. Gilje, R. B. Kaner and G. G. Wallace, *Nat Nano*, 2008, **3**, 101-105.
73 73. R. H. Müller, G. Hildebrand, R. Nitzsche and B.-R. Paulke, *PAPERBACK APV*, 1996, **37**.
74 74. A. Zintchenko, H. Dautzenberg, K. Tauer and V. Khrenov, *Langmuir*, 2002, **18**, 1386-1393.
75 75. V. Starchenko, M. Müller and N. Lebovka, *The Journal of Physical Chemistry C*, 2008, **112**, 8863-8869.
76 76. H. V. Sæther, H. K. Holme, G. Maurstad, O. Smidsrød and B. T. Stokke, *Carbohydrate Polymers*, 2008, **74**, 813-821.
77